Standard Issue – Article

Journal of Agricultural Engineering

https://www.agroengineering.org/

Development of a combined harvester navigation control system based on visual simultaneous localization and mapping-inertial guidance fusion

Fuhao Zhu, Jin Chen, Zhuohuai Guan, Yahui Zhu, Hao Shi, Kai Cheng

Publisher's Disclaimer

E-publishing ahead of print is increasingly important for the rapid dissemination of science. The *Early Access* service lets users access peer-reviewed articles well before print/regular issue publication, significantly reducing the time it takes for critical findings to reach the research community.

These articles are searchable and citable by their DOI (Digital Object Identifier).

Our Journal is, therefore, e-publishing PDF files of an early version of manuscripts that undergone a regular peer review and have been accepted for publication, but have not been through the typesetting, pagination and proofreading processes, which may lead to differences between this version and the final one.

The final version of the manuscript will then appear on a regular issue of the journal.

Please cite this article as doi: 10.4081/jae.2024.1583

©The Author(s), 2024
Licensee PAGEPress, Italy

Submitted: 26/07/2023
Accepted: 17/04/2024

Note: The publisher is not responsible for the content or functionality of any supporting information supplied by the authors. Any queries should be directed to the corresponding author for the article.

All claims expressed in this article are solely those of the authors and do not necessarily represent those of their affiliated organizations, or those of the publisher, the editors and the reviewers. Any product that may be evaluated in this article or claim that may be made by its manufacturer is not guaranteed or endorsed by the publisher.

Development of a combined harvester navigation control system based on visual simultaneous localization and mapping-inertial guidance fusion

Fuhao Zhu,[1] Jin Chen,[1] Zhuohuai Guan,[2] Yahui Zhu,[3] Hao Shi,[1] Kai Cheng[1]

[1]College of Mechanical Engineering, Jiangsu University, Zhenjiang, Jiangsu; [2]Nanjing Institute of Agricultural Mechanization, Ministry of Agriculture and Rural Development, Nanjing, Jiangsu; [3]Jiangsu World Agricultural Machinery Co. Danyang, Jiangsu, China

Correspondence: Jin Chen, College of Mechanical Engineering, Jiangsu University, Zhenjiang, Jiangsu, 212013, China.
E-mail: chenjinjd126@126.com

Key words: combine harvester; inertial guidance; navigation; SLAM; vision.

Acknowledgments: Demonstration and Promotion Project of Modern Agricultural Machinery Equipment and Technology of Jiangsu Provincial Department of Agriculture and Rural Affairs (NJ2022-08); Jiangsu Provincial Scientific and Technological Achievement Transformation Project (BA2020054); National Natural Science Foundation of China (52205272).

Conflict of interest: the authors declare no potential conflict of interest.

Abstract

Recently, the existing unmanned systems of combine harvesters mostly adopts satellite navigation scheme, lacking real-time observation of harvesting adjustment. To improve the operational efficiency of combine harvester assisted navigation operation, this paper designs a combine harvester navigation control system based on vision simultaneous localization and mapping (SLAM)-inertial guidance fusion. The system acquires field image information and extracts the crop boundary line as the navigation datum by binocular camera. First, the system acquires field image information through binocular camera and extracts the crop boundary line as the navigation datum. Second, fusing camera and inertial guidance information to obtain the real-time relative position of a combine harvester. Third, constrained optimization of image and inertial guidance information is achieved through a sliding window optimization method based on tightly coupled nonlinear optimization. Finally, obtain the position of the combine harvester relative to the navigation datum line, and output a signal to the steering mechanism to realize the combine harvester in the field intelligent positioning navigation control. The system consists of binocular camera, inertial measurement unit, motorized steering wheel, monitor display, angle sensor and microcontroller. During field testing, the system underwent repetitive harvesting trials over a distance of 25 m.. The testing machine performs field operations at a speed of 0.9-1.5 m/s, with an average lateral deviation range of 2.21-8.62 cm, a standard deviation range of 0.13-4.21 cm and an average cutting rate range of 92.2%-96.0%, achieving the expected harvesting effect.

Introduction

Information technology has gradually been applied to agricultural production with the increasing level of agricultural mechanization in the world. The use of navigation technology to enhance operational efficiency is gaining more attention in the operation of agricultural machinery. During the operation process, the driver must constantly adjust the forward direction of the combine harvester to ensure the full cutting width. This is due to the complexity of the field environment. During prolonged operation, the driver's attention may be diverted by the need to observe the crop boundaries of the cutting platform, which can pose a safety hazard to agricultural production. Therefore, studying navigation technology to assist the driver in controlling the machine's motion is crucial (Luo et al, 2016).

Currently, agricultural machinery primarily uses satellite navigation, visual navigation and inertial navigation (Tan et al, 2020; Zhang et al, 2020). With the advancement of agricultural machinery intelligence, the use of machine vision in agriculture has gradually matured, replacing human perception of the environment to a certain extent, and has become a focus of research (Yang and Li, 2021). The research on vision-based passive navigation technology (Zhu et al, 2011) for agricultural machinery can accelerate the development of unmanned agricultural machinery.

In recent years, numerous scholars worldwide have conducted extensive research on methods for positioning and navigation control of agricultural machinery. Robert et al (1996) from Stanford University, USA, were the first to equip a John Deere tractor with a GPS navigation system. The system had a straight-line tracking deviation of less than 2.5 cm; Cariou et al (2003) developed a navigation control system for agricultural machinery that uses a Kalman filter and a nonlinear speed control system. The system relies on RTK_GPS as a source of navigation control information; In Japan, Nagasaka et al (2010) and Yoshisada et al (2004) added a fiber-optic gyroscope to detect the forward direction of the vehicle while using GPS for positioning. The rice transplanter operated at a speed of 0.7 m/s in a paddy field and had a maximum lateral deviation of 12 cm, which satisfies the requirements for rice planting; Noguchi et al (2001) developed an agricultural tractor control system that utilizes multi-sensor fusion technology. The system uses sensors such as machine vision, gyroscopes, and GPS to address the issue of low GPS positioning accuracy caused by ground interference. Experiments indicate that the tracking error for localization of the trajectory is less than 5cm when moving forward at a speed of 2.2m/s; Ma et al (2019) built a low-cost navigation system based on machine vision and inertial sensors on a microcomputer, and estimated the navigation information by the extended Kalman algorithm, with a maximum error of ≤10 cm and a heading angle error of ≤1° during travelling; Zhang et al (2020) proposed a path detection algorithm for visually navigating jujube rows for date harvesting machines. The algorithm achieved an average path detection accuracy of 94%; The study above indicates that the machine's positioning primarily depends on satellite navigation, such as GPS and BeiDou. However, this method cannot determine the machine's relative position, and high-precision satellite navigation at the civilian level is expensive.

This study presents a combined harvester navigation control system that is based on vision SLAM-inertial guidance fusion. The system is designed to account for the motion characteristics of

wheeled combine harvesters and the accuracy of field positioning. The system integrates two types of sensor data from a binocular camera and an inertial measurement unit (IMU) (Li et al, 2016; Lu et al, 2016; Ma et al, 2020; Xu et al, 2021) to achieve sensor complementarity and obtain accurate and reliable real-time relative position information of the combine harvester. The steering mechanism of the combine harvester is adjusted based on the field data acquired, enabling auxiliary control and improving harvesting efficiency while reducing costs.

Materials and Methods

Scheme design of navigation control system of combined harvester

Navigation system hardware design composition

Due to the complex operating environment of the combine harvester, the navigation system must achieve position detection and boundary recognition of the body based on the harvester's different motion postures and the irregularity of the crop boundary. Process visibility, data storage, and read/write functions are necessary.

This paper presents the design of a navigation control system for a combine harvester using vision SLAM-inertial fusion, in accordance with the specified requirements. Figure 1 displays the system's hardware components. The system primarily comprises a binocular camera, an inertial sensor IMU, a rear wheel angle sensor, and a power control steering wheel. Binocular cameras, inertial sensors, and angle sensors are used for environmental awareness. The collected data is analyzed and processed by the system, which then transmits a control signal to the steering mechanism. The combine harvester's closed-loop steering control is achieved by using the actual steering angle of the rear wheels, which is fed back by the angle sensor.

Navigation algorithm framework design

Visual SLAM algorithms are mainly used for real-time positioning and map construction. The binocular inertial SLAM algorithm (Zhang et al, 2017) constructed in this paper has the following components:

(1) Front-end visual odometry. It mainly contains the extraction of the navigation boundary line of the combine harvester, the motion position estimation of binocular images, the preprocessing of IMU data and the visual inertial guidance data alignment.

(2) Back-end state estimation. It mainly contains reprojection error constraints for binocular vision, IMU pre-integration constraints, and optimal estimation of the combine harvester's position using nonlinear optimization and sliding-window construction of a least squares problem.

Figure 2 shows the algorithm's architectural flow. Firstly, the combined harvester's perception of the environment was acquired using a binocular camera and inertial IMU (Cheng et al, 2017). Secondly, Determine the position of the fuselage following sensor alignment and initialization. To select key frames, assuming that the number of feature points of the two images acquired by the left and right eyes of the binocular camera in the current frame is N, the number of road marking points in the point set of the local map is S, and the number of feature points in the current frame that have been successfully matched with the point set is T. Based on the motion conditions of the field operation, we make judgments on the ratios of T/N and T/S to complete the selection of key frames. Thirdly, Add filtered keyframes to the sliding window for optimization. The sliding window is used to maintain and optimize the information from the camera and inertial guidance due to the large deviation of acquired images and errors in position estimation. This ensures accurate airframe position information. Finaly, the steering angle information can be obtained by calculating the deviation between the navigation boundary line acquired by the binocular camera and the motion state prediction of the combine harvester. This allows for precise steering control of the combine harvester.

Dual front-end visual odometer

Binocular pose estimation and navigation boundary line extraction

The front-end of the SLAM algorithm obtains relative motion increments from image sequences captured by the binocular camera and extracts the positions of feature points in the world coordinate system w. The process can be divided into four main stages: feature detection and matching, correction and outlier rejection, kinematic position estimation, and triangulation measurement (Scaramuzza et al, 2011).

Figure 3 shows a schematic representation of the working principle of the binocular stereo vision front-end. First, extract the feature points and compute their descriptors to obtain the ensemble C_i of the roadmap points in space. The ensemble of projections of the feature points at the k-th moment is represented by $\{C_k^{Li}, C_k^{Ri}\}_{i1-3}$. The feature points are corrected using the OpenCV correction function.

This function performs binocular feature matching based on the similarity of the feature descriptors. The rejection of the dissimilarity point is then carried out; Second, The ISP method can be used to compute $\Delta T_{k-1,k}$ and $\Delta T_{k,k+1}$, which represent the incremental change in pose of two adjacent image sequences. This provides an estimation of the kinematic pose represented by the camera coordinate system; The camera's external reference matrices, T_k, T_{k+1} and T_{k-1}, represent the transformation of the world coordinate system w to the camera coordinate system. The waypoint's position in w can be obtained.

The navigation datum is the crucial foundation for the combine harvester navigation system's forward direction. Its basic principle is to extract the edge of the field crop to be harvested from the image as the navigation datum. The feature points and navigation reference line of the field are extracted using a binocular camera during the front-end visual odometer's pose calculation. Homomorphic filtering (Liang et al, 2010) is applied to the acquired images. Homomorphic filtering is a technique used in frequency domain processing to address the issue of non-uniform illumination in field images. The fundamental principle is to process the image through image frequency filtering and grayscale transformation. Various methods have been proposed to address the issue of uneven image illumination, including the gray-scale transformation method (such as the histogram equalization method), the illumination-reflection based homomorphic filtering method, the Retinex enhancement method, and the gradient-domain image enhancement method, etc (Liang et al, 2010). The illumination-reflection model views an image $f(x,y)$ as the product of the incident component $i(x,y)$ and the reflected component $r(x,y)$, as shown in Eq. 1.

$$f(x,y) = i(x,y) \cdot r(x,y) \tag{1}$$

The grayscale of the image is determined by the incidence and reflection functions. The incidence indicates the light conditions, which change slowly and are part of the low-frequency information barrenness. The reflection component represents the detailed part of the image, which changes rapidly and belongs to the high-frequency, information-rich portion of the image. During image pre-processing, the goal is typically to reduce low frequencies and increase high frequencies in order to preserve image details and improve overall quality.

Eq. 2 is obtained by performing a logarithmic operation on the original image $f(x,y)$ before performing homomorphic filtering.

$$lnf(x,y) = lni(x,y) + lnr(x,y) \tag{2}$$

Eq. 3 is obtained by performing the Fourier transform.

$$F(u,,v) = I(u,v) + R(u,v) \tag{3}$$

The incident and reflected components can be separated for subsequent filtering. After multiplying the homomorphic filtered transfer function $H(u,v)$ on both sides of Eq. 2, the Fourier inverse transform yields the spatial domain.

$$\mathrm{h_f}\,(\mathrm{x},\mathrm{y}) = \mathrm{h_i}\,(\mathrm{x},\mathrm{y}) + \mathrm{h_r}\,(\mathrm{x},\mathrm{y}) \tag{4}$$

Finally, the Eq. 3 is de-exponentiated to obtain the final image output $g(x,y)$.

$$g(x,y) = e^{h_f\,(x,y)} = e^{h_i\,(x,y)} \cdot e^{h_r\,(x,y)} \tag{5}$$

Pixel values near the edge of the crop are retained by removing some high-frequency noise through grayscaling and bilateral filtering after performing image illumination homogenization. Then, binary thresholding and morphological opening operations are applied to facilitate edge detection. Finally, after being processed by the Canny edge detection operator, the resulting image is subjected to the cumulative probability Hough transform. When calculating the direction and length of a line segment, only certain points in the plane are taken into account to reduce calculation time. Random sampling was used to select the points for straight line fitting. The procedure will terminate once the number of fits reaches the predetermined threshold. Figure 4 illustrates the result of the navigation boundary line detection procedure.

Inertial measurement unit inertial measurement unit pre-integral

The IMU (inertial measurement unit) includes three uniaxial accelerometers and three uniaxial gyroscopes that measure the angular velocity and acceleration of an object in three-dimensional space and use them to solve for the object's attitude. However, the output frequency is high and errors accumulate over time (Zhou et al, 2021; Liu et al, 2016). When processing IMU data, the frequency of inertial navigation measurements is several times higher than that of image acquisition, resulting in a high calculation cost. To reduce the amount of calculation, the IMU measurement model is pre-integrated (Lupton and Sukkarieh, 2011), and the IMU and camera data are aligned. Figure 5 shows the pre-integration schematic. Eq. 6 represents the pre-integration formula. Integrating all inertial measurement unit (IMU) data between frame k and frame $k+1$ provides the initial values for the position p, velocity v, and rotation q of frame $k+1$ for visual estimation. The time interval is represented by Δt, while a and ω represent the acceleration and angular velocity, respectively.

The calculation of the inertial guidance increment in the interval $[k, k+1]$ is the pre-integration of the IMU. The IMU state at moment k is known to have been obtained.

$$\begin{cases} p_{k+1} = p_k + v_k \Delta t + \frac{1}{2} a \Delta t \\ v_{k+1} = v_k + a \Delta t \\ q_{k+1} = q_k \otimes \begin{pmatrix} 1 \\ \frac{1}{2} \omega \Delta t \end{pmatrix} \end{cases} \tag{6}$$

Visual-inertial data fusion based on sliding window

The system acquires road marking points and inertial IMU data for positioning and navigation. The camera acquires key frames with timeliness due to the special characteristics of field operation. As a result, during combine harvester operation, crop feature points in the unharvested area disappear after harvesting. Additionally, during turning operations, when the environment changes significantly, feature points are easily lost. To address these issues, a sliding window based on the key frames is used to control the parameter optimization of the control system state variables (Qin et al, 2018) and to carry out the optimal estimation of the overall motion state of the combine harvester.

Before the final position optimization, it is necessary to initialize the sensor information. The bias and scale factors of the inertial sensors are estimated primarily through the rotation and translation matrices of the camera.

To construct a visual-inertial guidance system with accurate positioning and local consistency, we construct IMU residuals, marginalized residuals, and key-frame visual error terms in a sliding window to optimize the state variables during combine harvester operation. Eq. 7 below shows all the state variables in the window, which include all the camera states.

$$X = \left[x_0, x_{1,\ldots} x_n, x_c^b, \lambda_0, \lambda_1, \cdots \lambda_m\right] \tag{7}$$

$$x_k = \left[p_{b_k}^w, v_{b_k}^w, q_{b_k}^w, b_a, b_g\right] \tag{8}$$

$$x_c^b = [p_c^b, q_c^b] \tag{9}$$

The x_k includes the current position, velocity, orientation, accelerometer bias, and gyroscope bias as represented by the IMUs. The parameter x_c^b refers to the outer parameter of the camera system in relation to the IMU body system. The rotation and rotation matrices in x_c^b are represented by p_c^b and q_c^b respectively. λ_m represents the inverse depth of one of the 3D points.

Set the window's fixed keyframe to $N = 10$. After harvesting, the feature points of the original image have irreversibly disappeared. When new keyframes are added to the window, the oldest ones are deleted. The old keyframes pass on the camera and inertial guidance information to the remaining variables through marginal probabilities. Then, an objective function is constructed, and nonlinear least squares optimization is performed. Eq. 10 represents the least squares optimization equation.

$$\min_{\chi}\left\{\| r_p - J_p X \|^2 + \delta \sum_{k\in B} \| r_B\left(\hat{z}_{b_{k+1}}^{b_k}, X\right) \|^2_{\Sigma b_k b_{k+1}} + \tau \sum_{(l,j)\in C} \rho(\| r_c(\hat{z}_l^{c_j}, X) \|^2_{\Sigma_l^{c_j}})\right\} \tag{10}$$

The prior information $\| r_p - J_p X \|^2$ is obtained from the marginalized keyframes. The IMU residual is represented by $\sum_{k\in B} \| r_B(\hat{z}_{b_{k+1}}^{b_k}, X) \|^2_{\Sigma b_k b_{k+1}}$, while the visual residual is represented by $\sum_{(l,j)\in C} \rho(\| r_c(\hat{z}_l^{c_j}, X) \|^2_{\Sigma_l^{c_j}})$. The parameters δ and τ are used for adaptive adjustment.

When steering operations are detected, the camera information and inertial guidance information are adjusted for weighting due to the irreversible disappearance of image feature points. When removing the position and feature points of the old keyframes to calculate marginalized residuals, only the IMU constraint relations associated with them are retained. These are then transformed into a priori information of the system optimization. Non-linear optimization is then performed. Ultimately, the combine harvester's current bit position is output.

Steering controller design

To address the issue of front and rear wheel spacing and steering radius, we establish a motion model for a wheeled combine harvester, disregarding external factors such as wheel slip between tyres and the ground. The coordinate system $O_w - x_w - y_w$ is established with the right limit position of the cutting table, as shown in Figure 6. During harvesting operations, the combine harvester maintains a constant forward speed and faces the y_w direction. The parameters for threshing, cleaning, paddle wheel, and cutting table height are set beforehand. The actual cutting width is determined by subtracting the distance (h) from the crop boundary to the rightmost side of the cutting table from the actual maximum cutting width (F) of the cutting table. During operation of the auxiliary navigation control system, steering is adjusted to achieve full-width harvesting based on

the lateral deviation (h) between the current crop boundary line and the predicted direction of the fuselage movement. Eq. 11 represents the crop boundary line, which serves as the navigation datum.

$$\alpha x + \beta y + \gamma = 0 \tag{11}$$

When performing steering control, it is also important to monitor the heading angle. The speed can be calculated using the translation matrix between neighboring frames. The heading deviation angle (φ) can be calculated using the crop boundary line and the heading direction of the combine harvester. When performing harvesting as shown in Figure 6, Δφ can be expressed as Eq. 12.

$$\Delta\varphi = \arg\tan\left(\frac{\alpha}{\beta}\right) + \frac{\pi}{2} \tag{12}$$

By using the distance L from the rear wheel axle to the cutting table and the forward speed, it is possible to calculate the radius of movement R of the cutting table during steering, as well as the change in lateral deviation. Eq. 13 shows the calculation of the cut-amplitude G-transform based on the corresponding data.

$$\begin{cases} G = F - h \\ R = \dfrac{L}{\tan\theta} \\ h = R(1 - \cos\Delta\varphi) \end{cases} \tag{13}$$

L, distance from rear wheel axle to cutting table, m; R, turning radius, m; F, actual maximum cutting width, mm; h, lateral deviation, cm; θ,Rear Wheel Turning Angle, degrees (°); φ, Heading Deviation Angle, degrees (°);

To meet the requirements of the navigation control system, we selected a single neuron PID control algorithm for the steering control algorithm of the combine harvester. This algorithm aims to regulate the direction faster and more accurately. Figure 7 shows the block diagram of the control strategy. The control signal is output by the navigation control system based on the angle of the rear wheel steering input. The steering information is outputted to the steering wheel by the system. The motor is controlled by the steering wheel to adjust the rear wheel steering based on the signal. The combine harvester's steering control is achieved by using feedback from the rear wheel angle sensor. This ensures that the cutting deck's edge fits the crop boundary line for efficient harvesting and navigation control.

Results and Discussion

Field tests

Test data and operating environment

Field tests were conducted at Jiangsu Nianfeng Farm in Zhenjiang Danyang, Jiangsu Province, China to verify the operating effect of the combine harvester navigation control system designed in this paper. A navigation control system based on vision SLAM-inertial fusion was integrated into a Ward 4LZ-8F wheeled combine harvester. The harvester has a camera height of 3100 mm, a cutting deck width of 2600 mm, and a front/rear wheel spacing of 285 cm, as shown in Figure 8.

The accuracy and robustness of the entire system depend heavily on the vision sensor, which serves as the primary source of information acquisition. This paper uses MYNTEYE-S1030-IR standard version, the data output format is Raw, and the resolution is 752×480. The manufacturer of the products is MYNTAI, located in Beijing, China; The inertial measurement unit serves as an auxiliary camera to capture instantaneous motion states. It requires high sampling frequency and accuracy. This paper uses the WIT HWT901B inertial guide produced by WIT Intelligent Company in Shenzhen, China, which has a lower cost, and is able to record the motion status of the combine harvester in real time; The NVIDIA TX2 development board, manufactured by NVIDIA Corporation, headquartered in Santa Clara, California, USA, was selected for development. It has strong AI computing capabilities, 256 CUDA cores to accelerate graphics processing, and a multi-core CPU that is more suitable for multi-threaded operations throughout the program. The GTCV13609 is a contact shaft type angle sensor with a resolution accuracy of 0.022°.

Steering control test

Simulation of the controller is necessary when conducting field tests. First, conventional PID (Proportion Integration Differentiation) parameter tuning was performed. Then, the algorithm was validated in the Simulink environment by simulating a fixed lateral deviation input of 20 cm. It was discovered through continuous test parameters that the steering effect was superior when $K_p = 0.215$, $K_i = 9.236$, and $K_d = 0.071$; The tuning of parameters for the single neuron PID (Ding et al, 2020) primarily involves adjusting the learning rate and gain coefficient. By setting up the update state variables and adjusting the input and learning rate tuning parameters, we can obtain the final gain coefficient $K = 3.1$, as well as the learning rates $\mu_p = 16.2$, $\mu_d = 10.4$, and $\mu_i = 23.3$. Figure 9 displays the simulation data. To simulate sudden field conditions, increase the perturbation

at 6 seconds. Analysis shows that the single neuron PID control is superior and the designed system meets the auxiliary navigation control requirements of the combine harvester.

Fieldwork tests

To verify the combine harvester navigation control system's operating effect, we selected a conventional rice field for the accuracy test of the navigation system. We measured and analyzed the cutting width. Assessing the navigational quality of a combine harvester through lateral deviation and average cutting rate.

This is an example of path tracking for a straight-line harvesting operation of a combine harvester at an operating speed of $1.2m/s$. Figure 10 shows the effect of the trajectory of 25m straight line harvesting. GT in the illustration shows the crop edge of the test field's data localization using a high-precision handheld GPS as a comparison to the combine harvester's operating trajectory; The illustration shows that the system detects the driving trajectory. This track is recorded by the combine harvester's auxiliary navigation system. This is a coordinate transformation to derive the right limit trajectory of the cutting table, using the center axis trajectory as the reference; The illustration shows that GPS detects the driving track. It represents the trajectory left by the GPS as it moves with the combine harvester operation; The graph's origin represents the initial position of the machine, with the Y-axis indicating forward distance and the X-axis indicating lateral movement. Figure 11 shows the difference in coordinates between the actual movement trajectory and the crop boundary line. This represents the lateral deviation of the combine harvester. Eq. 14 is used to calculate the lateral deviation.

$$\Delta l = |l_s - l_z| \tag{14}$$

In Eq. 14, Δl represents the lateral deviation, l_s represents the system's detected traveling trajectory, and l_z represents the crop edge.

The perimeter of the field should be trimmed to enable the harvester to make turns during wheeled combine operations. Based on the data presented in Figure 10, the mean lateral deviation was calculated to be 5.89 cm, with a standard deviation of 0.04 cm. The system is more robust, and the combine harvester can operate more effectively along the boundary line under the navigation control system. Figure 12 displays the cutting width variation curve. The average cutting width is 239.6cm with a standard deviation of 2.3cm, resulting in an average cutting width rate of 95.8%. The

nominal cutting width of the combine harvester is 260cm, while the maximum cutting width during actual operation is 250cm. This satisfies the system design requirements.

To compare the effect of navigation control accuracy under different operating states and speeds, we conducted repeated tests at 0.9m/s and 1.5m/s. The combine harvester navigation operation test included straight lines and irregular curves. The specific test results are shown in Table 1.

The comparative test data from the three groups show that when the combine harvester operates at low speed $0.9m/s$ and medium speed $1.2m/s$, the average cutting rate is similar. However, at high speed $1.5m/s$, the average cutting rate decreases significantly. Therefore, to ensure higher harvesting efficiency, the combine harvester should maintain a speed of about $1.2m/s$.

Conclusions

This paper presents a navigation control system designed for the specific characteristics of combine harvester field operation, based on binocular SLAM-inertial fusion. The binocular camera is used to obtain real-scale information and motion position. Inertial guidance can assist the camera in obtaining more accurate scale information, speed, position transformation, and other data. The combination of the two sets of data can be optimized to determine the relative position of the combine harvester in the field. The designed steering controller can accurately adjust the motion attitude of the combine harvester so that the combine harvester can maintain a high cutting width and harvesting efficiency.

The test results indicate that, under the condition of no leakage, the navigation control system integrated test prototype developed in this paper can effectively ensure that the cutting width rate meets the actual operational requirements when the combine harvester operates at a speed of 0.9~1.5m/s. The average cutting width rate ranges from 92.2% to 96.0%, the average transverse deviation ranges from 2.21 to 8.62cm, and the standard deviation ranges from 0.13cm to 4.21cm. The system can more accurately measure the positional transformation of the harvester and compensate for any deviation in the forward path or crop harvesting boundary. This allows for adjustment of the steering mechanism to achieve full-width operation requirements and meet the efficiency standards of the combine harvester's passive automatic navigation harvesting.

References

Campos C, Elvira R, JJG Rodríguez, et al. ORB-SLAM3: An Accurate Open-Source Library for Visual, Visual-Inertial and Multi-Map SLAM[J]. 2020.

Cariou C, Berducat M, Lenain R, et al. Automatic Guidance of Farm Vehicles[J]. Springer Netherlands, 2003.

Cheng Chuanqi, Hao Xiangyang, Li Jiansheng, et al. Monocular visual-inertial navigation based on nonlinear optimization[J]. Journal of Chinese Inertial Technology, 2017,25(05):643-649. (in Chinese with English abstract)

DAVID B, BEN U, GORDON W, et al. Vision-based obstacle detection and navigation for an agricultural ro-bot[J]. Journal of Field Robotics, 2016, 33(8): 1107-1130.

Ding Youchun, Xia Zhongzhou, Peng Jingye, et al. Design and experiment of the single-neuron PID navigation controller for a combine harvester[J]. Transactions of the Chinese Society of Agricultural Engineering (Transactions of the CSAE), 2020, 36(7): 34-42. (in Chinese with English abstract) doi: 10.11975/j.issn.1002-6819.2020.07.004 http://www.tcsae.org

Liu Yang, Gao Guoqin. Research Development of Vision-based Guidance Directrix Recognition for Agriculture Vehicles[J]. Journal of Agricultural Mechanization Research, 2015,37(05):7-13. DOI: 10.13427/j.cnki.njyi.2015.05.002. (in Chinese with English abstract)

LI Fengyang, JIA Xue-dong, DONG Ming. Development of vision/inertial integrated navigation in different application scenarios[J]. Journal of Navigation and Positioning,2016,4(4):30-35. DOI:10.16547/j. cnki. 10-1096. 201 60406.

Li Guojun, Xu Yanhai, Duan Jiewen ,et al. ORB-SLAM method based on local adaptive threshold extraction feature points[J]. Bulletin of Surveying and Mapping,2021(9):32-36,48. (in Chinese with English abstract)

Liang Lin, He Weiping, Lei Lei, et al. Survey on enhancement methods for non-uniform illumination image[J]. Application Research of Computers, 2010,27(05):1625-1628. (in Chinese with English abstract)

Liu M, Chang G. Numerically and statistically stable Kalman filter for INS/GNSS integration[J]. Proceedings of the Institution of Mechanical Engineers, Part G: Journal of Aerospace Engineering, 2016.

Luo Xiwen, Liao Juan, Hu lian, et al. Improving agricultural mechanization level to promote

agricultural sustainable development[J]. Transactions of the Chinese Society of Agricultural Engineering(Transactions of the CSAE) 2016，32(1)： 1-11.

Lu Jianjun, Rwn Xiaojun，Sun Wei, et al. INS /Stereo Visual Odometry Deeply Integrated Navigation Method[J]. Navigation Positioning and Timing,2016,3(03):37-43. (in Chinese with English abstract)

Ma Xianglu, Yao Xiaoshan, Ding Rensong. Influence of IMU's quality on VIO: based on MSCKF method[J]. SIXTH SYMPOSIUM ON NOVEL OPTOELECTRONIC DETECTION TECHNOLOGY AND APPLICATIONS,2020,11455.

Ma Zhiyan， Ouyang Fangxi， Yang Guangyou, et al. Research on Multi－Sensor Integrated Navigation Based on Vision and Inertia[J]. Journal of Agricultural Mechanization Research, 2019, v.41(06):13-18. (in Chinese with English abstract)

Meng Qingkuan, Qiu Ruicheng, Zhang Man, et al. Navigation System of Agricultural Vehicle Based on Fuzzy Logic Controller with Improved Particle Swarm Optimization Algorithm[J]. Transactions of the Chinese Society for Agricultural Machinery, 2015,46(03):29-36+58. (in Chinese with English abstract)

Mur Artal Raul and Tardos Juan D. ORB-SLAM2: An Open-Source SLAM System for Monocular, Stereo, and RGB-D Cameras[J]. IEEE Transactions on Robotics, 2017, 33(5): 1255-1262.

Nagasaka Y, Saito H, Tamaki K, et al. An autonomous rice transplanter guided by global positioning system and inertial measurement unit[J]. Journal of Field Robotics, 2010, 26(6-7): 537-548.

Noguchi N, Qin Z, Han S, et al. Autonomous Agricultural Tractor with an Intelligent Navigation System[J]. IFAC Proceedings Volumes, 2001, 34(19): 197-202

Qin Tong and Li Peiliang and Shen Shaojie. VINS-Mono: A Robust and Versatile Monocular Visual-Inertial State Estimator[J]. IEEE Transactions on Robotics, 2018, 34(4): 1004-1020.

Robert P C, Rust R H, Larson W E, et al. Automatic Steering of Farm Vehicles Using GPS[M]. Proceedings of the Third International Conference on Precision Agriculture, 1996.

SCARAMUZZA D, FRAUNDORFER F. Visual odometry [Tutorial] [J]. IEEE Robotics & Automation Magazine,2011,18(4):80-92.

Shufeng H, Qin Z, John F. Reid. A Navigation Planner for Automatic Tractor Guidance Using Machine Vision and DGPS[J]. IFAC Proceedings Volumes,2001,34(09): 209-214.

Tan Chenjiao，Li Yilin，Wang Dongfei，et al. Review on Automatic Navigation Technologies of Agricultural Machinery[J]. Journal of Agricultural Mechanization Research,2020,42(05):7-14+32. DOI: 10.13427/j.cnki.njyi.2020.05.002. (in Chinese with English abstract)

T. Lupton, S. Sukkarieh. Visual-inertial-aided navigation for high-dynamic motion in-built envi-ronments without initial conditions[J]. IEEE Transactions on Robotics, 2011, 28(1): 61-76

Vision-based Obstacle Detection and Navigation for an Agricultural Robot[J]. Journal of Field Robotics, 2016, 33(8): 1107-1130.

XU Zhibin,LI Hongwei, ZHANG Bin, et al. Localization method of mobile robot based on binocular vision and inertial navigation[J]. Acta Geodaetica et Cartographica Sinica,2021,50(11):1512-1521. DOI:10.11947/j. AGCS.2021.20210250.

Yang Tao, Li Xiaoxiao. Research progress of machine vision technology in modern agricultural production [J]. Journal of Chinese Agricultural Machinery,2021,42(3):171-181(in Chinese with English abstract)

Yoshisada, Nagasaka, And, et al. Autonomous guidance for rice transplanting using global positioning and gyroscopes[J]. Computers & Electronics in Agriculture, 2004.

Zhang Man，Ji Yuhan，Li Shichao，et al. Research Progress of Agricultural Machinery Navigation Technology[J]. Transactions of the Chinese Society for Agricultural Machinery, 2020,51(04):1-18. (in Chinese with English abstract)

Zhu Z S, Yuan C Z, Zhou P. Situation and development of passive navigation localization technology. Progress in Geophys. (in Chinese), 2011, 26(4):1473~ 1477, DOI: 10. 3969/j. issn. 1004-2903. 2011. 04. 044. (in Chinese with English abstract)

Zhang Xiongchu, Chen Bingqi, Li Jingbin, et al. Path detection of visual navigation for jujube harvesters[J]. Transactions of the Chinese Society of Agricultural Engineering (Transactions of the CSAE), 2020, 36(13): 133-140. (in Chinese with English abstract)

Zhang Guoliang，Yao Erliang1，Lin Zhilin,et al. Fast Binocular SLAM Algorithm Combining the Direct Method and the Feature-based Method[J]. Robot, 2017,39(06):879-888. (in Chinese with English abstract)

Zhou Silong, Liang Dong, Wang Hui, et al. Remote Sensing Image Segmentation Approach Based

on Quarter-tree and Graph Cut[J]. Computer Engineering,2010,36(08):224-226. (in Chinese with English abstract)

Zhou H, Zhong Y, Song H, et al. Gyro-Free Inertial Navigation Technology[J]. 2021.

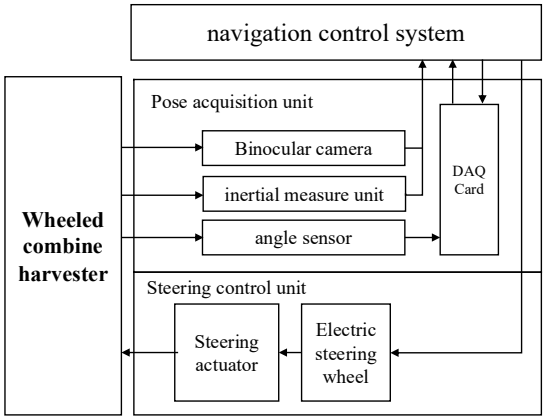

Figure 1. Block diagram of hardware components.

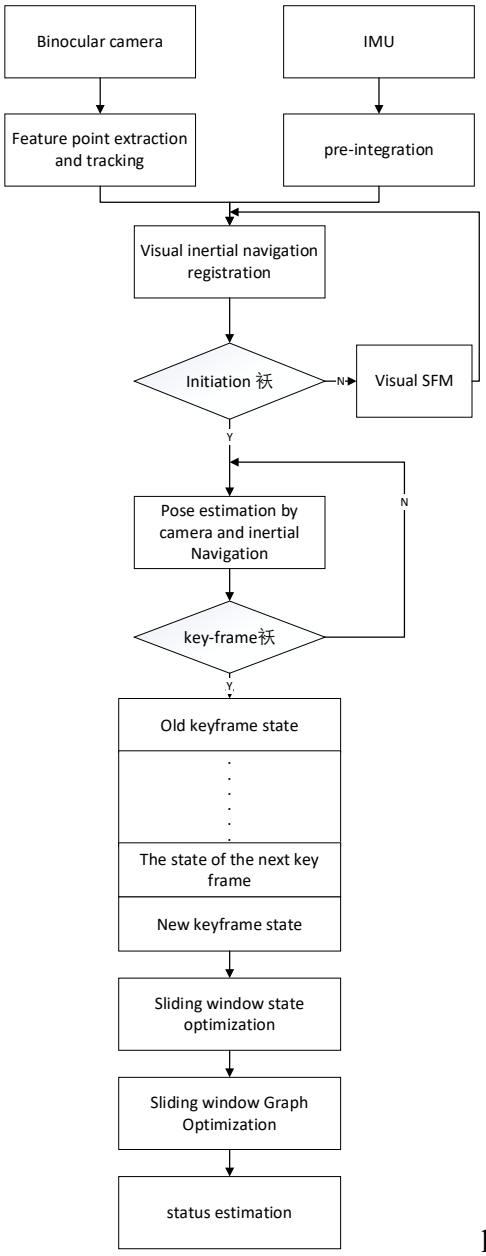

keyframe 不清楚

Figure 2. SLAM algorithm system block diagram.

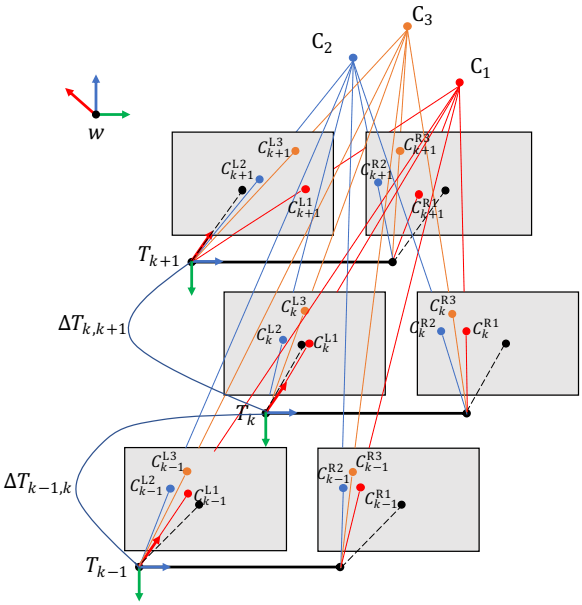

Figure 3. The schematic diagram of binocular VO front-end.

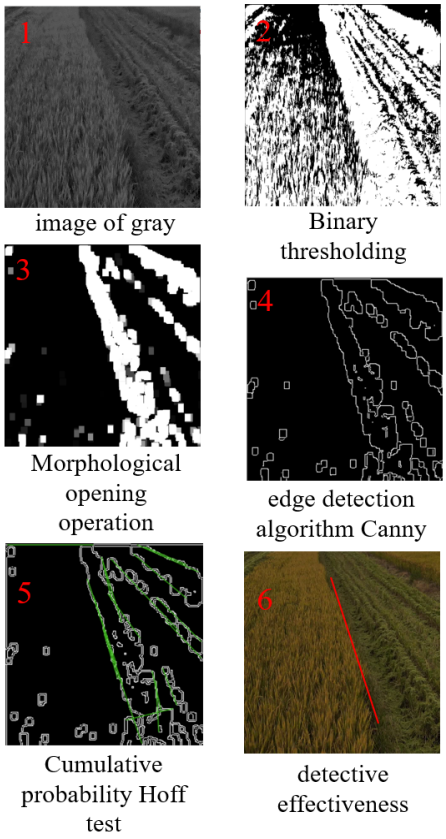

Figure 4. Rendering of navigation boundary line detection program.

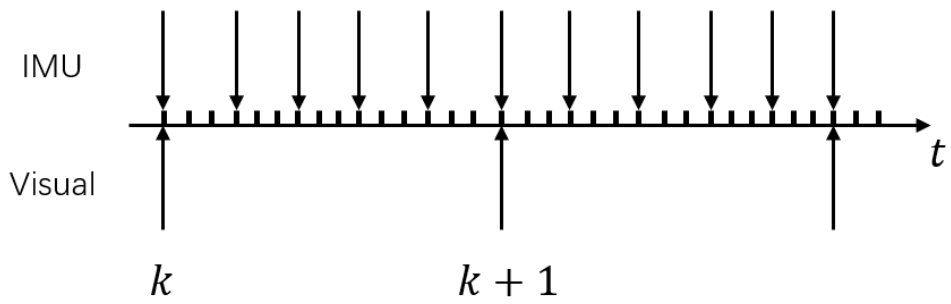

Figure 5. Schematic diagram of pre-integration.

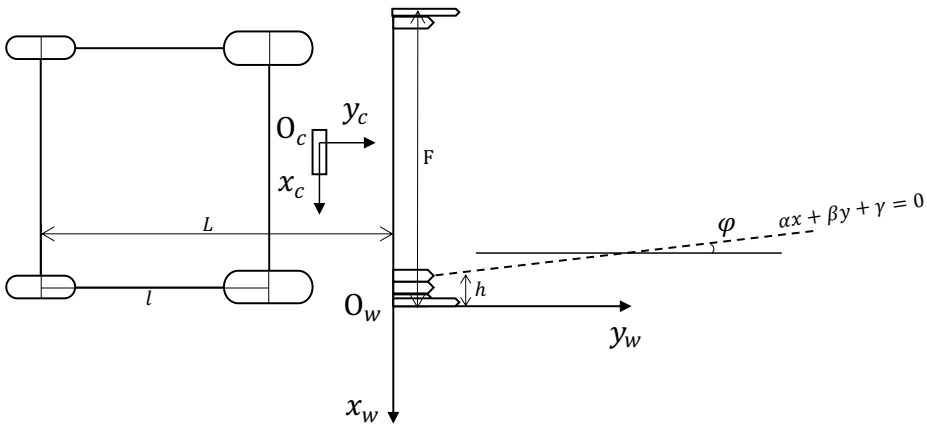

Figure 6. Motion model of wheeled combine harvester.

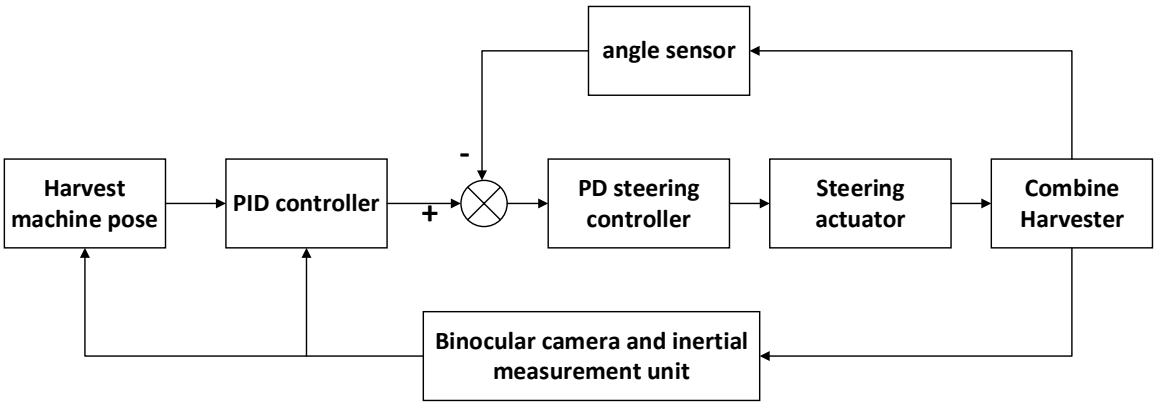

Figure 7. Assisted navigation control strategy diagram.

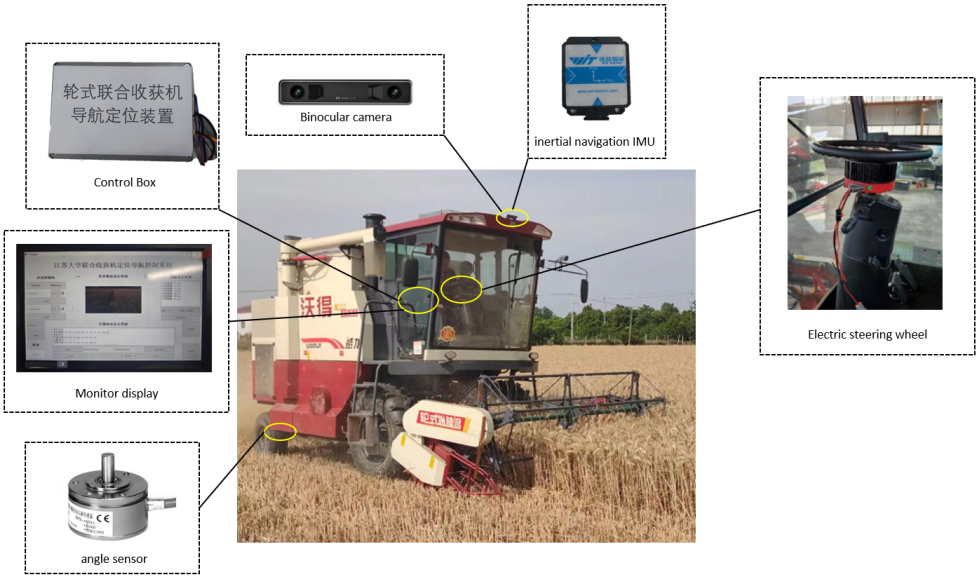

Figure 8. Test platform.

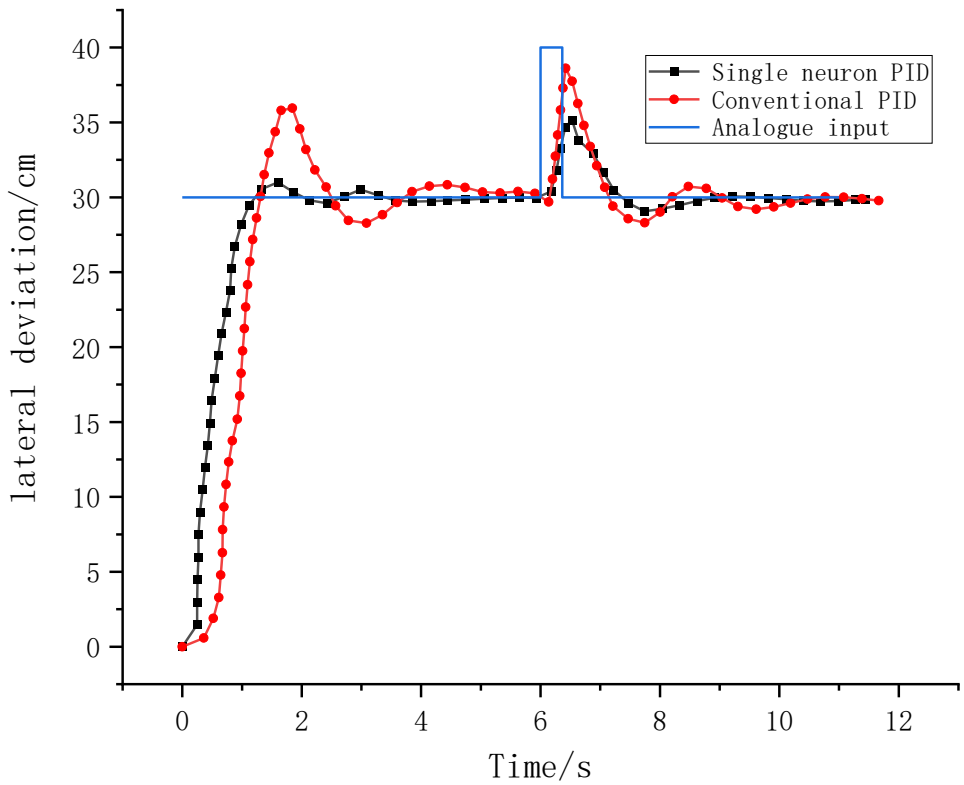

Figure 9. Steering control simulation adjustment diagram.

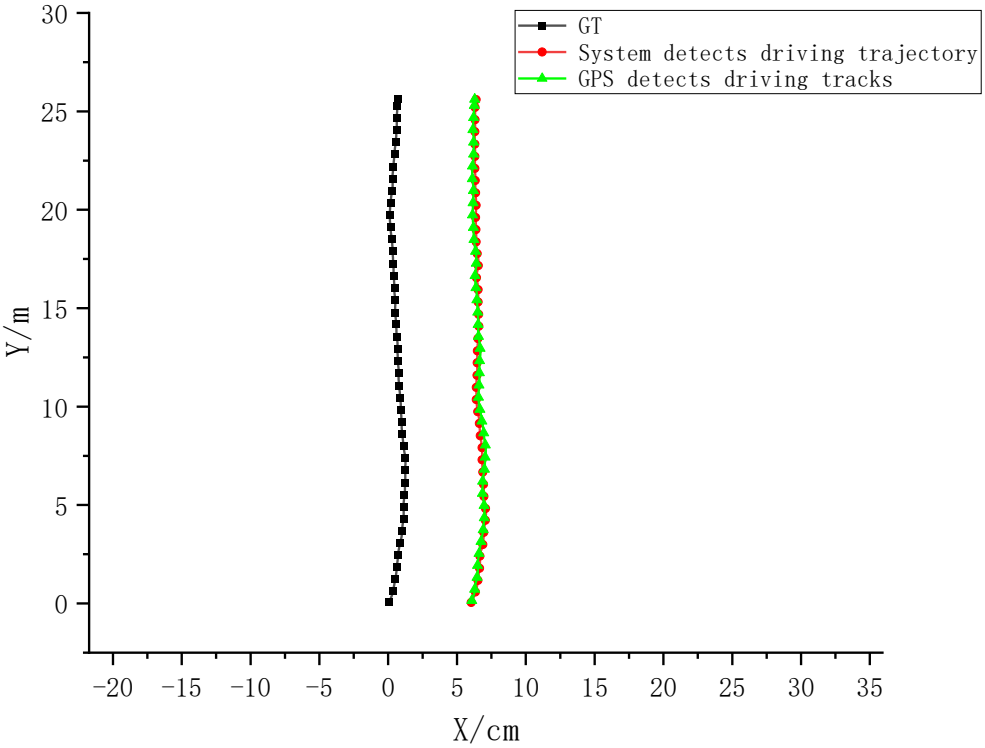

Figure 10. Comparison chart of job trajectories.

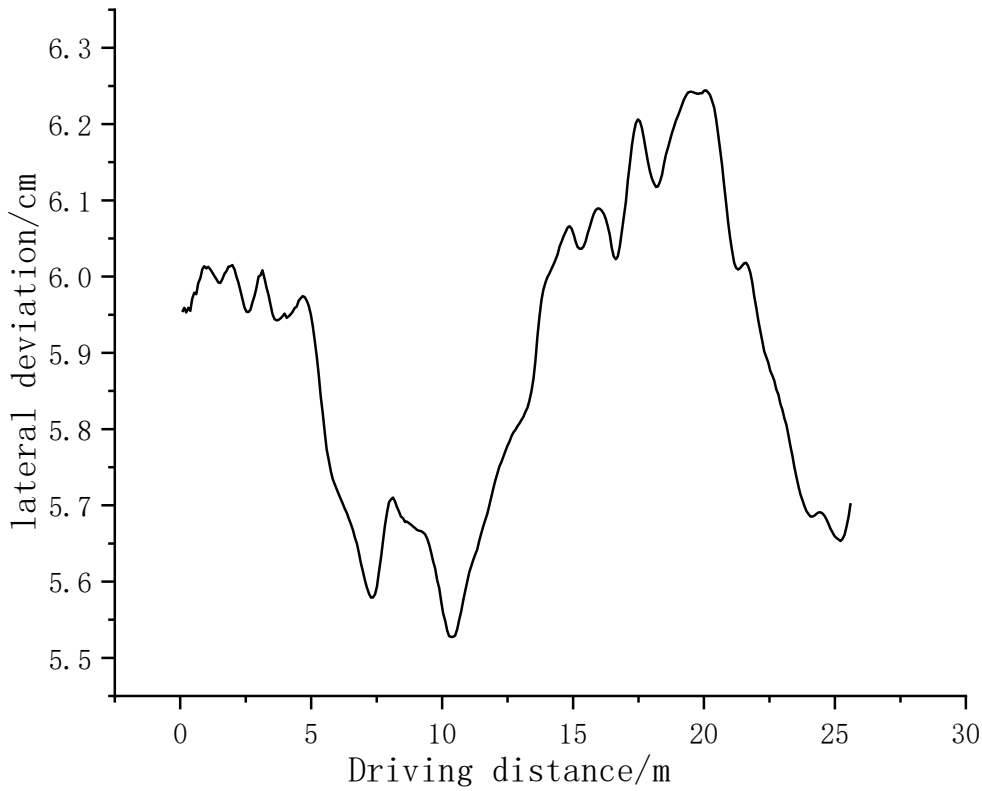

Figure 11. Horizontal deviation diagram.

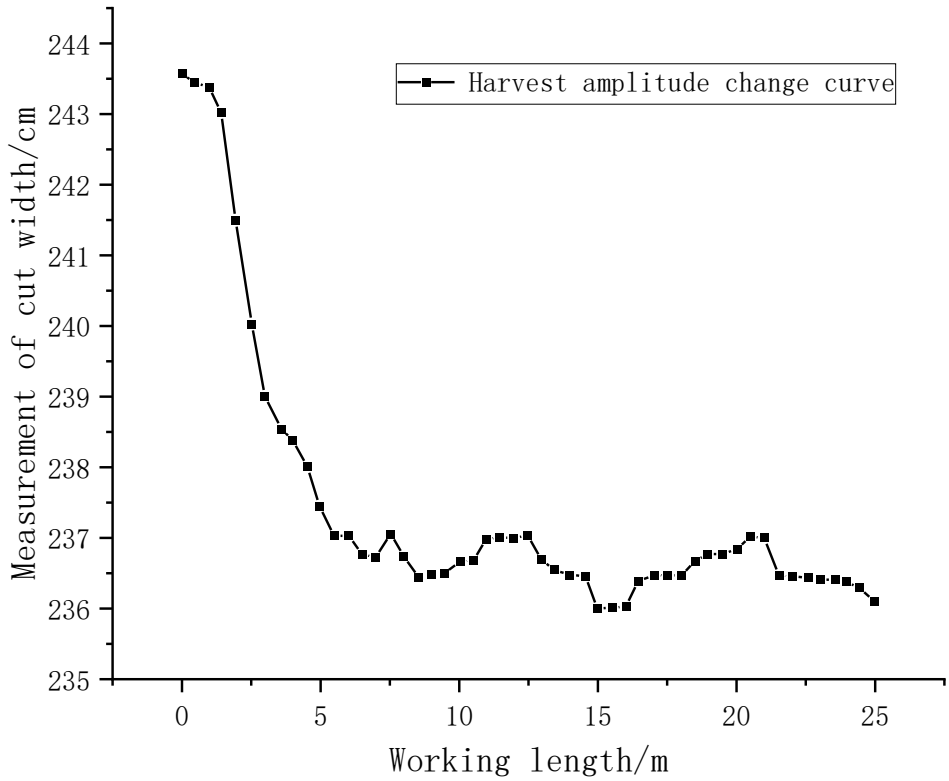

Figure 12. Actual cutting measurement data of linear operation.

Table 1. The results of field navigation experiments.

Operating speed (m/s)	Operating environment	Mean lateral deviation (cm)	Lateral deviation standard deviation (cm)	Actual cut width (cm)	Average cut rate (%)
0.9	Line work	2.21	0.13	240.1	96.0
	Irregular curve	4.31	1.92	239.8	95.9
1.2	Line work	5.89	0.24	239.6	95.8
	Irregular curve	3.34	2.18	237.4	94.9
1.5	Line work	7.33	1.64	232.5	93.0
	Irregular curve	8.62	4.21	230.6	92.2